



## SOURCE, PATH AND SITE EFFECTS IN THE EPICENTRAL AREA OF THE 1997-98 UMBRIA MARCHE SEQUENCE (CENTRAL ITALY)

Bindi D. <sup>1</sup>, Castro R. R. <sup>2</sup>, Franceschina G. <sup>1</sup>, Luzi L. <sup>1</sup>, Marzorati, S. <sup>1</sup> and Pacor F. <sup>1</sup>

### SUMMARY

The simulation of deterministic scenarios needs the knowledge of spectral parameters of seismic sources, propagation and site transfer functions. The results of this study represent the estimates of the spectral parameters characterizing the ground motion from weak to moderate earthquakes in the Umbria-Marche area (Central Italy). This region was recently struck by a seismic sequence that started on September 1997 and ended on June 1998. The whole seismic sequence consisted of several moderate magnitude earthquakes ( $M_w$  6) that ruptured normal faults oriented along the main trend of the Central Apennines. We analyzed strong-motion spectra recorded during the sequence using a non parametric inversion. We found that the attenuation can be described by the frequency dependent quality factor  $Q(f) = 49f^{0.9}$  up to 8 Hz and  $Q = 318$  at frequencies higher than 8 Hz and by the geometrical spreading  $G(r) = r^{-0.9}$ . The source spectra are omega-square shaped with an average stress drop equal to  $(2 \pm 1)$  MPa. Since strong site effects were recognized for most of the analyzed stations, the simulation of deterministic scenarios should account for site amplification. Therefore the validity of the site transfer functions was checked through standard methods such as horizontal to vertical spectral ratios HVRS and 1D propagation models of S waves through horizontally stratified soil columns. The different techniques provided consistent results, both in shape and amplitude, except for those stations located on deep alluvium basin where 2D effects cannot be neglected. The spectral parameters obtained with the inversion have been used to simulate the strong motions recorded during several events occurred in the area using point source and finite fault models.

### INTRODUCTION

The synthesis of strong ground motion over the entire frequency range of engineering interest requires the knowledge of the rupture mechanism controlling the seismic energy radiated from the source, the effect of wave propagation and the response of the near surface soil layers.

Our study provides the estimates of source, attenuation, and site spectral parameters using strong motion data recorded in the epicentral region of the 1997 - 1998 Umbria - Marche (central Italy) sequence. The new calibration of spectral parameters specific for this area is then used for predicting the effects of

---

<sup>1</sup> Istituto Nazionale di Geofisica e Vulcanologia, Sezione di Milano, Via Bassini 15, 20133 Milano, Italy.

<sup>2</sup> CICESE, Departamento de Sismología, División Ciencias de la Tierra, Km 107 Carretera Tijuana-Ensenada, Baja California, 22860 México

moderate earthquakes ( $M < 6.0$ ) through the simulation of strong motion records. Predictive relations for PGA and PGV are obtained from the stochastic point source simulations [8; 9]. Our results allow a better definition of the seismic hazard in this region, which is one of the most risky in Italy.

There are several studies on earthquake spectral parameters of the Umbria-Marche area, hereafter referred to as UMA, that were based either on weak motion data or on analog strong motion records from different tectonic regions [25; 20; 19; 12; 6]. In this work we exploit a large strong motion data set available after the 1997-1998 Umbria-Marche seismic sequence and a collection of reliable geological-geotechnical information on the accelerometric sites. We analyze about 150 strong motion records from 25 stations operating in the area during the 14 strongest events ( $4.6 \leq M \leq 5.9$ ) of the 1997-1998 sequence. Records from other two past earthquakes that occurred in the same area ( $M$  5.9 and  $M$  5.2) complemented the data set. We apply a generalized inversion technique to obtain source, attenuation and site functions [11]. The validity of the site transfer functions is verified by comparing horizontal to vertical spectral ratios and one-dimensional theoretical models [16; 29], which are important to assess the limits of applicability of the empirical techniques [7].

The source spectra, the anelastic attenuation term, and the site transfer functions are then used for simulating the strong ground motions recorded during several events, using point source [8; 9] and finite fault models [21; 22]. Finally, attenuation relationships valid in UMA are derived, simulating peak ground acceleration and peak ground velocity at fixed magnitudes and distances for rock and soft site conditions.

## SEISMIC SEQUENCE

The seismic sequence started on 4 September 1997 with a  $M_w$  4.5 earthquake located at the boundary of the Umbria and Marche regions. Figure 1 shows the distribution of the epicenters of the strongest events of the sequence and Table 1 lists the epicentral parameters of the earthquakes analyzed.

**Table 1: list of the analyzed events**

| Earthquake | dd.mm.yy | hh:mm | Lat.   | Long.  | $M_l$ | H<br>[km] | $M_o$<br>[N m] | $\Delta\sigma$<br>[MPa] |
|------------|----------|-------|--------|--------|-------|-----------|----------------|-------------------------|
| 115        | 19.09.79 | 21:35 | 42.730 | 12.960 | 5.9   | 6.0       | 7.0E+17        | 1.94                    |
| 174        | 29.04.84 | 05:02 | 43.250 | 12.520 | 5.2   | 7.0       | 3.4E+17        | 1.03                    |
| 290        | 26.09.97 | 00:33 | 43.021 | 12.888 | 5.6   | 3.8       | 4.0E+17        | 2.28                    |
| 286        | 26.09.97 | 09:40 | 43.023 | 12.847 | 5.9   | 6.5       | 1.2E+18        | 2.85                    |
| 350        | 03.10.97 | 08:55 | 43.034 | 12.842 | 5.4   | 5.7       | 8.6E+16        | 2.58                    |
| 291        | 06.10.97 | 23:24 | 43.015 | 12.843 | 5.5   | 7.0       | 1.7E+17        | 4.26                    |
| 352        | 07.10.97 | 01:24 | 43.010 | 12.783 | 4.6   | 10        | 2.3E+15        | 2.77                    |
| 353        | 07.10.97 | 05:09 | 43.010 | 12.848 | 4.8   | 10        | 6.7E+15        | 3.19                    |
| 355        | 12.10.97 | 11:08 | 42.911 | 12.950 | 5.3   | 2.2       | 7.8E+16        | 0.90                    |
| 292        | 14.10.97 | 15:23 | 42.915 | 12.930 | 5.6   | 4.9       | 3.4E+17        | 1.01                    |
| 358        | 16.10.97 | 12:00 | 43.034 | 12.890 | 4.6   | 2.0       | 3.9E+15        | 1.29                    |
| 360        | 09.11.97 | 19:07 | 42.854 | 12.999 | 4.9   | 2.0       | --             | --                      |
| 362        | 21.03.98 | 16:45 | 42.951 | 12.914 | 4.6   | 4.1       | 4.0E+16        | 0.76                    |
| 363        | 26.03.98 | 16:26 | 43.191 | 12.886 | 5.6   | 47.0      | 1.2E+17        | 1.15                    |
| 364        | 03.04.98 | 07:26 | 43.184 | 12.759 | 5.0   | 2.6       | 5.7E+16        | 1.81                    |
| 365        | 05.04.98 | 15:52 | 43.190 | 12.773 | 4.7   | 5.4       | 1.9E+16        | 1.36                    |

The main events occurred on 26 September 1997: a  $M_l$  5.6 earthquake (event 290) at 0:33 GMT followed soon after by a  $M_l$  5.9, at 9:40 GMT, that represents the main shock of the seismic sequence (event 286). On 14 October, at 15:23 GMT, an earthquake of  $M_l$  5.6 (event 292) occurred to the south of the mainshock. More than 2000 shocks were recorded during the months that followed and, in particular,

several  $M_1 > 4.5$  events struck the area in April - May 1998. Among these earthquakes, the strongest one ( $M_1$  5.6, event 363) was located at the considerable depth of about 47 km [24].

The events can be associated with a NW-SE elongated fault zone with length of about 40 km [1]. The three largest shocks ruptured different segments of the fault zone (Figure 1) at shallow depth (5 - 7 km). Moment tensors show normal faulting mechanisms with NW-SE tension axes [15], in agreement with the aftershock depth distribution that defines a SW dipping plane.

The faulting mechanisms of the sequence fit well with the known seismotectonic regime of the central Apennines, a region characterized by frequent moderate magnitude earthquakes generated by normal faulting.

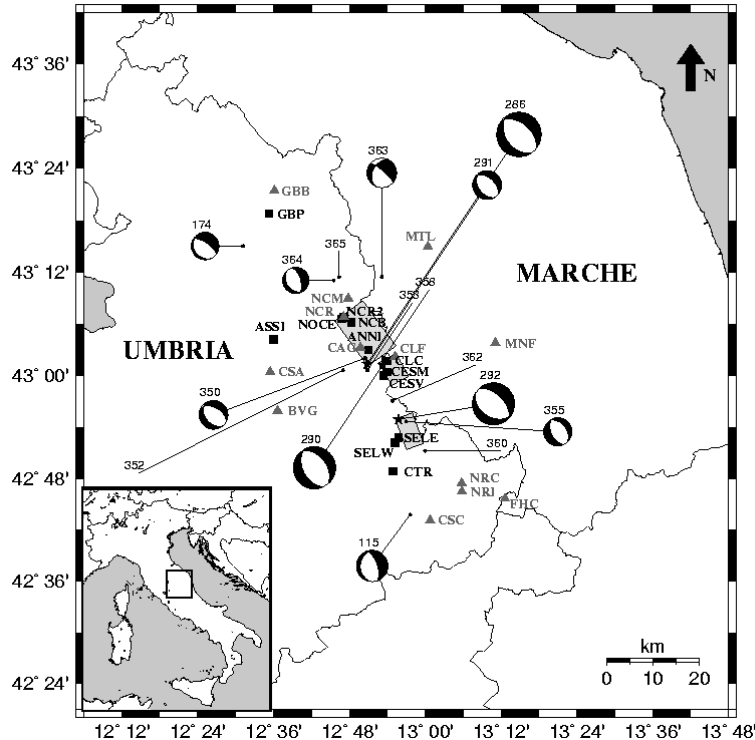


**Figure 1. Location of the main events and recording sites; focal mechanisms for events with  $M_1 > 5$  are shown. Squares and triangles represent digital and analog stations respectively.**

## DATA

We used about 150 strong motion records from 16 moderate ( $4.6 \leq M \leq 5.9$ ) earthquakes occurred in the Umbria Marche area during the 1979, 1984 and 1997-98 seismic sequences [28; 2]. We selected 25 sites for which reliable geological, geomorphological and geotechnical information were available. Recording sites were classified as follows: A) lacustrine and alluvial deposits with thickness  $> 30$  m; B) lacustrine and alluvial deposits with thickness  $< 30$  m; C) shallow debris or colluvial deposits (3-6 m) overlying rock; D) rock. Figure 1 shows the location of recording sites and the epicenters of selected earthquakes. Hypocentral distances range between 5 and 70 Km, although most of data have distances less than 40 Km. Accelerometric records were obtained from the National Strong Motion Network (RAN) managed by National Seismic Survey (SSN) and SOGIN (formerly Italian Electrical Company, ENEL), and from 10 mobile stations installed by SSN after the 26 September 1997 earthquake. Additional recordings were from permanent stations managed by ENEA (National Energy Agency). RAN stations were mainly

equipped with analog Kinometrics SMA1, having natural frequencies of 18 or 25 Hz and 0.5 or 1 g full scale. The set of mobile stations consists of 2 analog instruments of the same kind and 12 digital Kinometrics ETNA or K2 with natural frequency of 50 Hz and 1 g full scale. All of the records had a sampling rate of 200 samples per second. Analog records were base-line corrected and deconvolved for the instrument response. A zero-phase band pass filter was applied in order to reduce the noise content of data. On the average, analog records were band-pass filtered between 0.5 and 25 Hz.

The time window used for data analysis starts before the S-wave arrival and ends when 80% of the total energy is reached. A two sided 5% cosine taper were applied on selected windows and the FFT were computed. Spectra were smoothed using a variable frequency band, selected to preserve the energy, of  $\pm 25\%$  of 19 predefined frequencies between 0.4 - 18 Hz.

## METHOD

The generalized inversion technique (GIT) [4; 11] is adopted to separate the contributions of source, propagation and site of the observed spectra. The recorded spectral amplitude  $U(f,r)$  at frequency  $f$  and hypocentral distance  $r$  is described by the following predictive equation:

$$\text{Log}U(f,r) = \text{Log}S(f) + \text{Log}A(f,r) + \text{Log}Z(f) \quad (1)$$

where  $S(f)$  is the source spectrum,  $A(f,r)$  accounts for propagation effects, and  $Z(f)$  is the amplitude site transfer function. Given a set of earthquakes  $S_j, j=1\dots N_{ev}$ , and a set of recording stations  $Z_i, i=1,\dots,N_{sta}$ , a linear system is given from equation (1):

$$\text{Log}U_{ij}(f,r_{ij}) = \text{Log}S_j(f) + \text{Log}A(f,r_{ij}) + \text{Log}Z_i(f) \quad (2)$$

where  $A(f,r_{ij})$  is the spectral amplitude of event  $j$  recorded at station  $i$ . We solved system (2) following a two-step non parametric scheme [11]:

$$\text{Log}U_{ij}(f,r_{ij}) = \text{Log}\tilde{S}_j(f) + \text{Log}A(f,r_{ij}) \quad (3)$$

$$R_{ij}(f,r_{ij}) = \text{Log}S_j(f) + \text{Log}Z_i(f) \quad (4)$$

where  $\tilde{S}(f)$  is a scalar which depends on the source.

We solved the linear system (3) for different fixed frequencies  $f$  to determine the spectral attenuation with distance  $A(f,r_{ij})$  avoiding any parametric description. Once the spectral attenuation is determined, the residual  $R_{ij}(f,r_{ij})$  in system (4) is computed by correcting the amplitude data with  $A(f,r_{ij})$ . The solution of (4) allows us to isolate the source amplitude spectrum  $S(f)$  from the amplitude site transfer function  $Z(f)$ . For each considered frequency, both (3) and (4) are solved in a least-squares sense, by applying the LSQR method [23].

The solution of systems (3) and (4) generally requires some additional constraints to fix unresolved degrees of freedom. In solving system (3), we require that the attenuation is equal to 1 at the reference distance of 5 km. In system (4) we assume a reference site constraining its transfer function to an a-priori known function of frequency. This assumption makes all the others transfer functions relative to the assumed reference.

System (3) is solved in the range 5 to 61 km, using 28 distance intervals 2 km wide. We also smooth  $A(f,r_{ij})$  assuming a small second derivative. The systems (3) and (4) are solved for 19 frequencies in the range 0.4 - 18 Hz.

## RESULTS

### Source and attenuation term

The inversion scheme allowed us to obtain the spectral parameters that describe attenuation, source and site behavior. We describe the spectral attenuation with distance  $A(f, r_{ij})$  in terms of geometrical spreading and anelastic attenuation as:

$$A(f, r_{ij}) = \frac{5}{r_{ij}^n} \exp\left[-\frac{\pi f(r-5)}{Q(f)\beta}\right] \quad (5)$$

where  $\beta$  is the shear wave velocity. For each frequency, the geometrical spreading coefficient  $n$  and the quality factor  $Q(f)$  are estimated by fitting a straight line to  $\text{Log}A(f, r_{ij})$ . The best line has slope proportional to  $Q^{-1}$  (Figure 2c) and its intercept gives  $n$  (Figure 2b).

The quality factor shows a linearly increase with frequency and it can be approximated by  $Q(f) = 49 f^{0.9}$  at frequencies lower than or equal to 8 Hz; at frequencies greater than 8 Hz,  $Q$  becomes constant with an average of 318 (Figure 2c). A peculiar trend of  $A(f, r_{ij})$  is the slope change at distances larger than 40 km, that can be attributable to the arrival of Moho-reflected phases. Other authors [13] have already observed this phenomenon in the UMA .

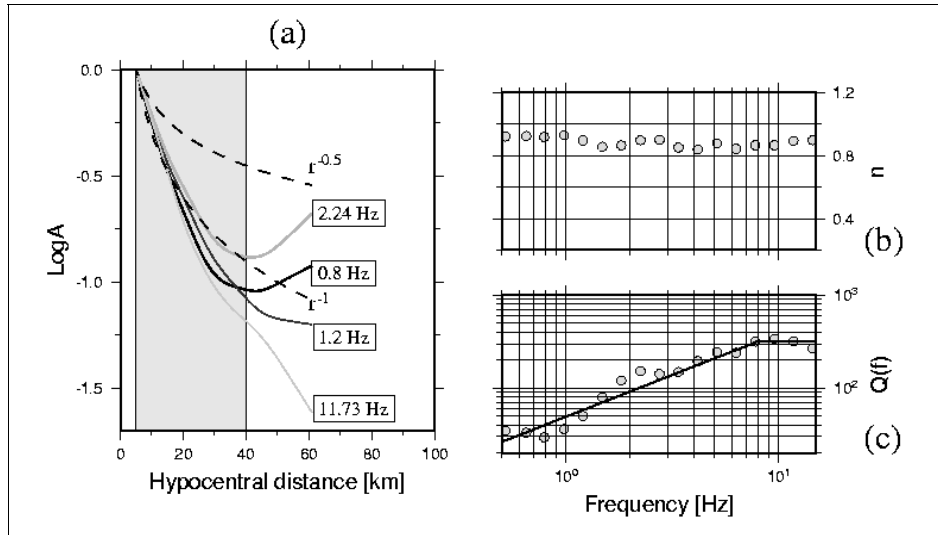


**Figure 2. Attenuation parameters: a) spectral attenuation versus distance for a sample of frequencies; b) geometrical spreading exponent versus frequency; c) best fit for Q factor.**

Source and site terms are obtained simultaneously by inverting the observed spectral amplitudes corrected for the attenuation functions computed in the first inversion step. The resulting source functions are then fitted to the  $\omega$ -square source model [10] to retrieve the source parameters. To avoid the trade-off between seismic moment  $M_0$  and corner frequency  $f_c$ , the fit is performed using the seismic moment values reported in the literature (Table 1), that allowed to constrain the corner frequency by the whole spectrum and in particular by the high frequency level (Figure 3). Generally, earthquakes having  $M < 5$  are well described by the  $\omega$ -square source model, whereas stronger events show lack of fit at low frequency (events 290, 291).

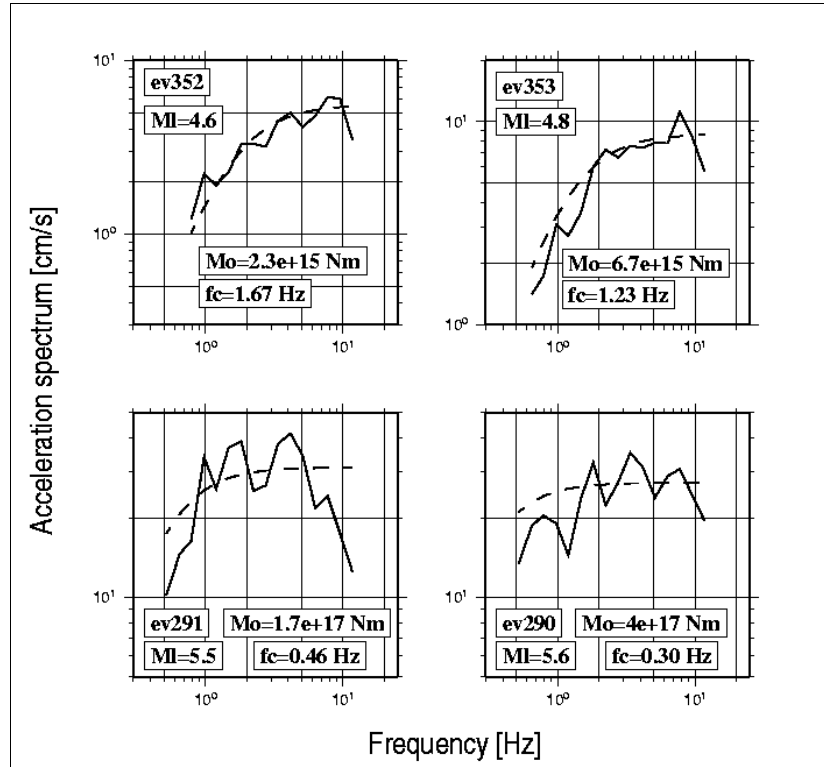


**Figure 3: Example of source spectra: continuous lines are inversion results, dashed lines are  $\omega$ -square model fits.**

Assuming a circular crack model, the source radius  $R_0$  and the stress drop  $\Delta\sigma$  are computed according to Brune [2]. Table 1 lists the estimated stress drop values, which range from 0.8 to 4.2 MPa. The average computed stress drop is  $\Delta\sigma = (2 \pm 1)$  MPa. This value agrees with the previous estimates by [6] obtained from the S-wave spectral analysis of about 500 weak motions ( $M < 4.5$ ).

### Site response

In the inversion procedure, site and source terms were separated by constraining the reference site function to the horizontal to vertical spectral ratios, HVRS, computed at the site ASSI using S-waves from 50 records. The accuracy of the reference transfer function cannot be directly assessed, because we lack detailed information to compute a theoretical site response. However, we have indirectly tested the reference site reliability by comparing the results of the generalized inversion and 1D modeling obtained at other two stations (CLF and MTL), where geotechnical profiles are available [7].

The site transfer functions obtained inverting equation (4) have been compared with those estimated using HVRS [17; 18]. Figure 4 displays the comparison between the two techniques for the stations representative of groups A, B, C, and D. The fundamental frequency of resonance estimated by both methods is consistent, with the exception of class A sites.

Stations belonging to class B have amplifications that never exceed a value of 3. No defined fundamental frequency is detectable and HVSR standard deviations are large. The obtained transfer functions for class C stations, located on shallow alluvial covers, are shifted towards higher values than class A, in the range 2 to 10 Hz, while amplitudes can reach a factor 5. Finally, class D stations show significant amplifications when they are installed on complex topography, while all the other sites have amplifications in the range 2-3.

In general, the largest amplifications for class A sites occur at low frequencies, in the range 0.5 - 2 Hz, where amplitudes reach a factor of 20. Most of class A sites are located on large sedimentary basins filled with an alternation of sandy-clayey deposits, that are typical in this region. The main cause of amplification is the occurrence of 2D effects, such as the generation of surface waves at the edge of these structures, that implies the presence, in the selected windows, of Rayleigh waves as shown for station GBP in Figure 5a. The analysis of different windows can thus lead to different results in terms of site transfer functions. Figure 5b also shows the two transfer functions at GBP obtained by adopting two different selection criteria: the 80% energy and the selection of a 5 s time window containing mainly S-wave arrivals. The resonant peak exhibits a strong decrease when the 80% energy criterion is adopted. For these sites, the corresponding HVSR underestimate the level of amplification compared to the generalized inversion. This feature is explained by the vertical component amplification, that invalidates the fundamental assumption of the HVSR method [14].

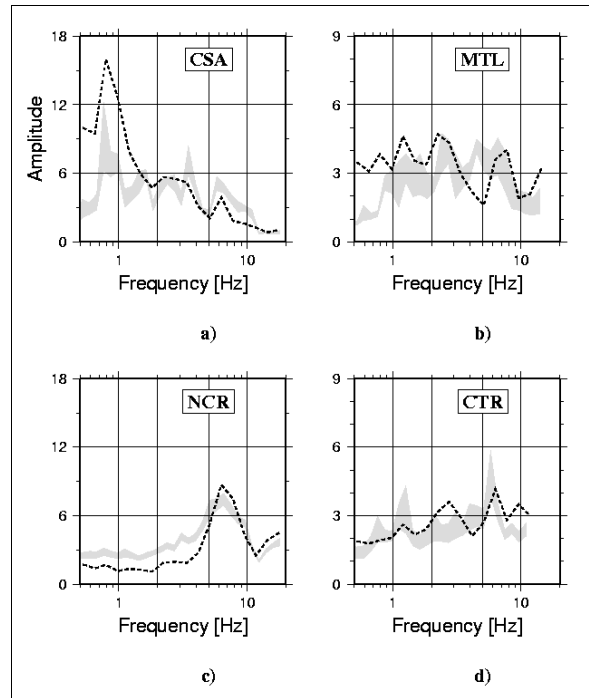


**Figure 4: Site transfer functions as HVSR  $\pm$  1std (gray shaded areas) compared to inversion results (dashed lines). Stations CSA, MTL, NCR and CTR are representative of class A, B, C and D sites respectively.**

## SIMULATIONS

The strong motions recorded during several events occurred in the UMA were simulated using the attenuation function  $A(f, r)$ , the source spectra  $S(f)$  and the site transfer functions  $Z(f)$ , obtained from the inversion. The standard point source approach proposed by Boore [8; 9] was adopted to generate synthetic seismograms at the recording stations triggered by events with  $M_1 < 5$  or located far from the source. The seismic moments  $M_o$  were taken from the literature (Table 1), while the attenuation parametric curve described as  $Q(f) = 49 f^{0.9}$  for  $f \leq 8$  Hz, and  $Q = 318$  when  $8 < f \leq 18$  Hz was assumed. In order to account for an unresolved contribution of the site at high frequency in the inversion, we introduced the spectral decay parameter  $k$  according to the model by Anderson and Hough [3]. An average spectral parameter  $k = 0.01$ s common to all stations was assumed to better reproduce the spectral amplitude decrease.

The uncertainty in the stress drop estimate was introduced by considering the mean  $\pm 1$  standard deviation. In Figure 6 the comparison between horizontal simulated and observed spectra is shown at some stations triggered by the events 352 ( $M_1 = 4.6$ ) and 363 ( $M_1 = 5.6$ , at hypocentral depth  $H=47$  km). The simulated spectra fit reasonably well the observations, showing that the source and attenuation models are suitable to describe the strong motion recorded in UMA.

Strong phases of the recorded accelerations, corresponding to the S-wave arrivals are also well reproduced both in amplitude and frequency content. The site term enclosed in the spectral model allows to adequately fit the spectral content of the signals, as demonstrated by the comparison between the recorded waveforms at CESV and NCR2, located at the same distance (about 50 km) from event 363. The same feature is apparent from waveforms comparison at stations ASSI and NCR2, located at slightly different distances (19 and 15 km, respectively) from event 352.

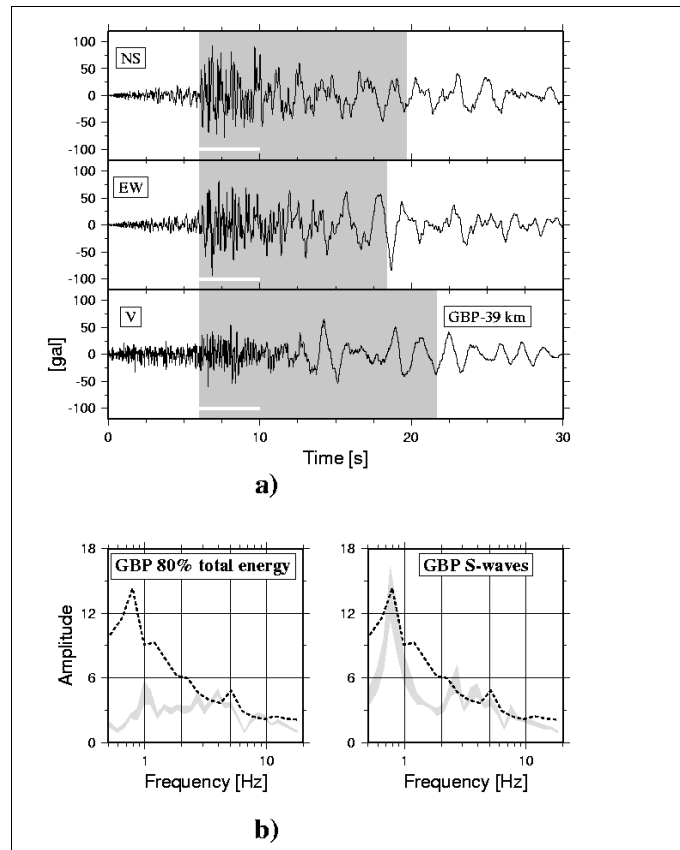


**Figure 5: Influence of windows selection in the HVSr analysis: a) observed acceleration at GBP (event 286); windows selected with the 80% energy criterion are gray shades, S-wave windows are underlined by the white line; b) 95% confidence limits of HVSr (gray areas) compared to the generalized inversion results (dashed lines).**

A model that takes into account the finite fault effects was used to simulate the event 292 ( $M_1 = 5.6$ ), one of the strongest of the sequence. The proposed approach is a deterministic-stochastic method [21; 22], hereafter referred to as DSM. This method extends the classic point-source stochastic method [8; 9] by including the effects of rupture propagation over a finite fault. The synthesis of any time history can be summarized as a four step procedure: a) generation of an acceleration envelope radiated from an extend fault with a simple kinematic rupture description through the isochron theory [5; 27]; b) windowing of Gaussian white noise time series with the deterministic envelope of point (a); c) transformation of the

windowed noise time history into the frequency domain and multiplication with a reference amplitude spectrum, whose parameters, i.e. corner frequency and distance from the fault, are evaluated through the kinematic model; d) transformation back to the time domain. The source spectrum is described with an omega-square model, parametrized by the apparent corner frequency,  $f_a$ , instead of standard corner frequency  $f_c$ . The apparent corner frequency varies from site to site and it is computed by the isochron theory as the inverse of the apparent duration of rupture,  $T_a$ , as perceived by the receiver. This approach makes the corner frequency independent of the seismic moment and stress drop, as the duration is a function of the fault dimensions, nucleation point and rupture velocity. Since the DSM assumes a source model independent of the Brune's stress drop, it allows to verify whether the  $Q(f)$  and  $k$  estimated by GIT are affected by a trade-off with the source term.

The DSM simulations were carried out using seismic moments reported in the literature, and adopting the same site terms and attenuation as in the stochastic point source simulations. In Figure 7, the comparison between simulated and recorded spectra and time histories (acceleration and velocity) are shown at 3 stations (CAG0, NCR2, CESM). On average the synthetic spectra reproduce, in shape and amplitude, the observed ones, confirming that the attenuation and site terms can be used independently of the source parameters. Both recorded acceleration and velocity time histories are reproduced reasonably well, thus allowing to be confident on the obtained strong ground motion simulations over the entire engineering frequency band.

A further application of the GIT results was the adoption of the source, path and site parameters obtained by the non parametric inversion to predict peak ground motion in the UMA, using the Boore's point source stochastic technique [8; 9]. The results were then compared with the peak ground acceleration and velocity obtained from the empirical attenuation relationships based on the Italian strong motion data-set [26], hereafter referred to as SP. Attenuation relationships were computed by simulating point sources with magnitudes in the range 4 - 6 for stations located on rock sites (class D) and on deep alluvium (class A). Computation was performed at fixed distances (from 5 to 50 Km).

The reason for the selection of class A sites lies in the similarity with class 2 of the SP attenuation relationship and in the high level of amplification characteristic of deep sedimentary basins in the UMA which could strongly influence the spectral content of ground motion.

The relationships that fit the synthetic data for class A sites are:

$$\begin{aligned} \log PGA &= -1.75 + 0.45M - 1.51 \log R_{hypo} \pm 0.18 \\ \log PGV &= -1.16 + 0.68M - 1.4 \log R_{hypo} \pm 0.2 \end{aligned} \quad (6)$$

where  $M$  is the local magnitude and  $R_{hypo}$  is the hypocentral distance; the relationships obtained for rock sites are:

$$\begin{aligned} \log PGA &= -1.46M + 0.38M - 1.57 \log R_{hypo} \pm 0.12 \\ \log PGV &= -0.88 + 0.57M - 1.4 \log R_{hypo} \pm 0.15 \end{aligned} \quad (7)$$

Mean values are plotted in Figure 8, together with SP attenuation curves for two events of  $M = 5.6$  and  $M = 5.9$ . The observed peaks recorded in UMA are also shown (events 286 and 115 for  $M = 5.9$ ; events 290, 292 and 363 for  $M = 5.6$ ). In general, the peak ground motions calculated by (6) have a stronger decay with distance than the SP predictions. The mean PGA's predicted by (6) and (7) are always lower than the ones predicted by SP. A similar trend is observed for the PGV of rock sites, whereas soft sites show larger values than SP at short distances ( $R < 30$  km). The PGV predictive relations are within the mean  $\pm 1$  standard deviation of the attenuation laws reported by Sabetta and Pugliese [26].

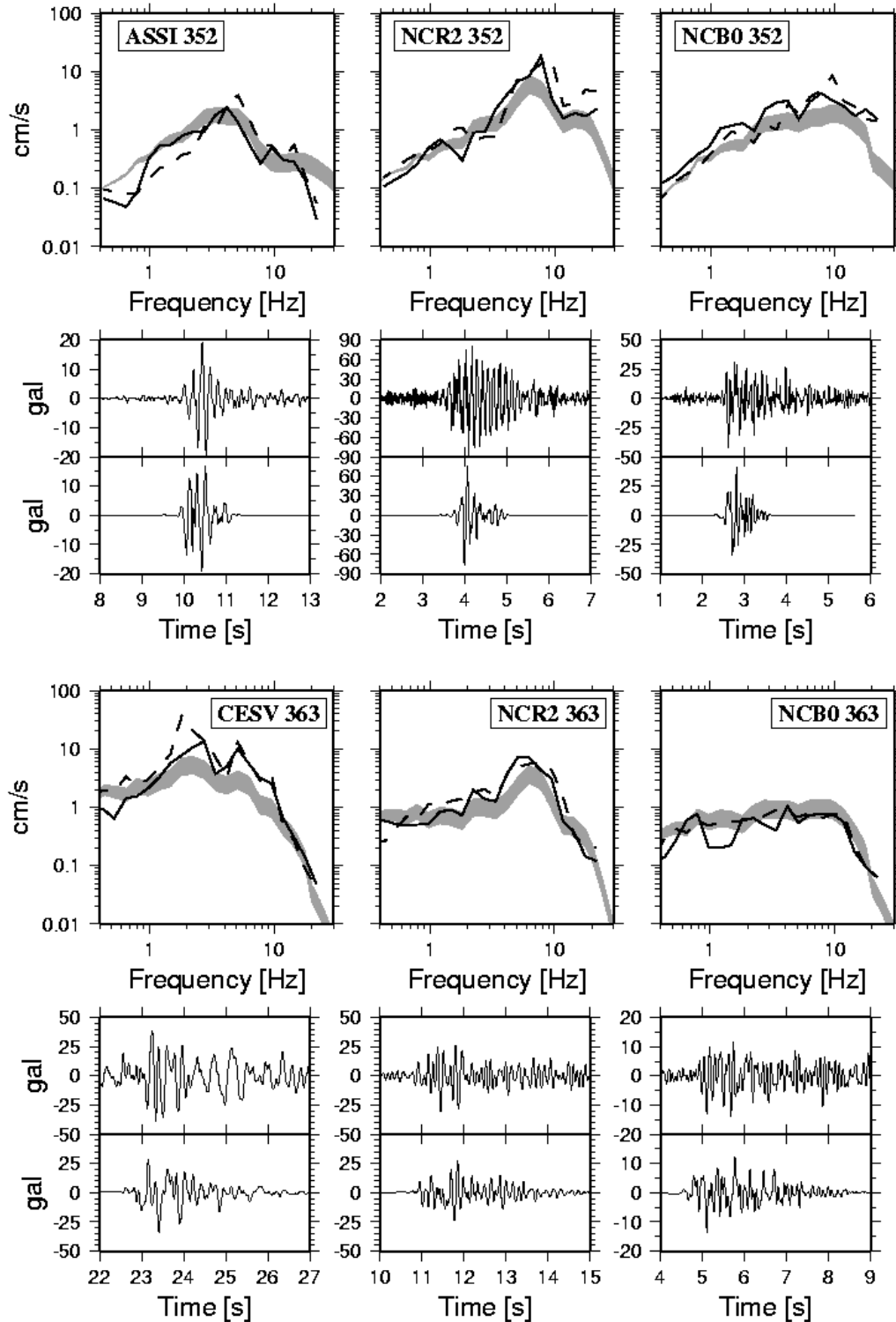
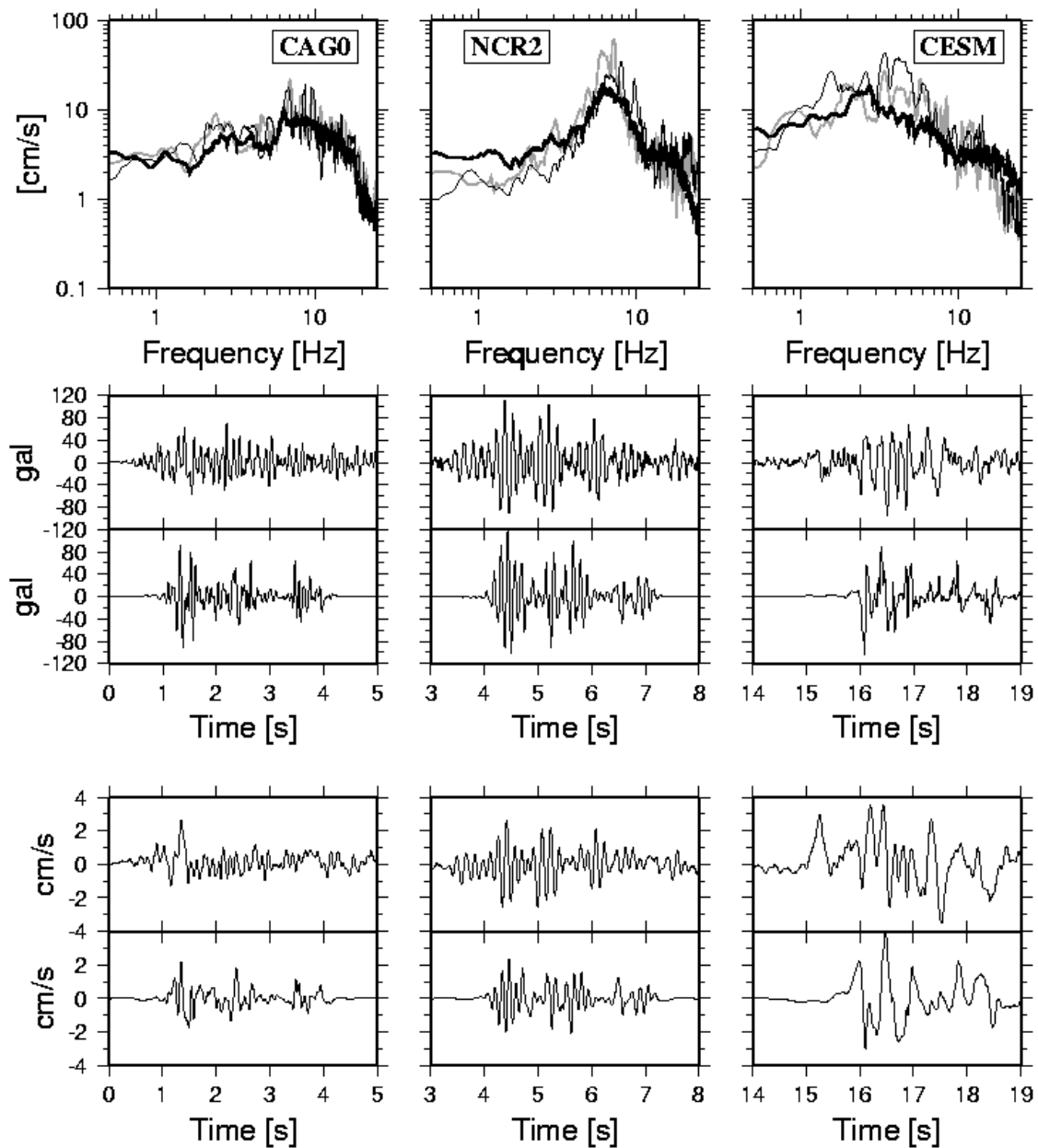


Figure 6: Acceleration spectra and acceleration time-histories for  $M_1 = 5.6$  events and 4 stations: continuous and dashed lines of the spectra are the two observed components, gray shaded areas are the simulated spectra assuming  $\Delta\sigma = (2 \pm 1)$  MPa; observed time histories are plotted above the simulated ones.



**Figure 7: Finite fault simulations with DSM (event 292, stations CAG0, NCR2, CESM); top panel: acceleration spectra (thick black is simulation; thin grey and black are observations); middle panel: acceleration time-histories (top observed, bottom simulated); bottom panel: velocity time-histories (top observed, bottom simulated).**

## CONCLUSIONS

The data set used in this study permit us reach the following goals: 1) to derive non-parametric functions that describe the crustal attenuation in the distance interval 5 - 40 km; 2) to define the source parameters in the magnitude range from 4.5 to 6; and 3) to represent site effects for different soil types.

The point source simulation results and the finite fault modeling confirm that the generalized inversion provides estimates of attenuation and site terms that can be used, independently of the source model, for predicting strong ground motion in UMA.

Several results should be highlighted. First of all the relevance of the site effects in the observed strong motion data, that should be accounted for whenever hazard-oriented studies are performed in UMA. This can be achieved through a detailed geological, geomorphological and geotechnical characterization of the recording sites. A set of attenuation parameters has been derived for regional hazard studies in the UMA, valid up to 40 km of hypocentral distance, beyond which post-critical reflected waves can significantly increase the acceleration spectral ordinates. The average stress drop proposed by this study agrees with that reported in the literature for similar tectonic regimes.

We propose a spectral attenuation model in UMA described by: i) quality factor  $Q(f) = 49 f^{0.9}$  for  $0.4 < f \leq 8$  Hz and  $Q = 318$  for  $f > 8$  Hz; ii) geometrical spreading  $G(r) = r^{-0.9}$  in the distance range  $5 < r < 40$  km; iii) high frequency decay parameter  $k = 0.01$  s. This model can be used to predict weak to moderate seismic ground motion at bedrock sites. As far as the source parameters are concerned, the stress drop  $\Delta\sigma = (2 \pm 1)$  MPa is adequate to successfully simulate the ground motions observed in Umbria - Marche Area during the 1997- 1998 seismic sequence, provided that the site effects are properly taken into account.

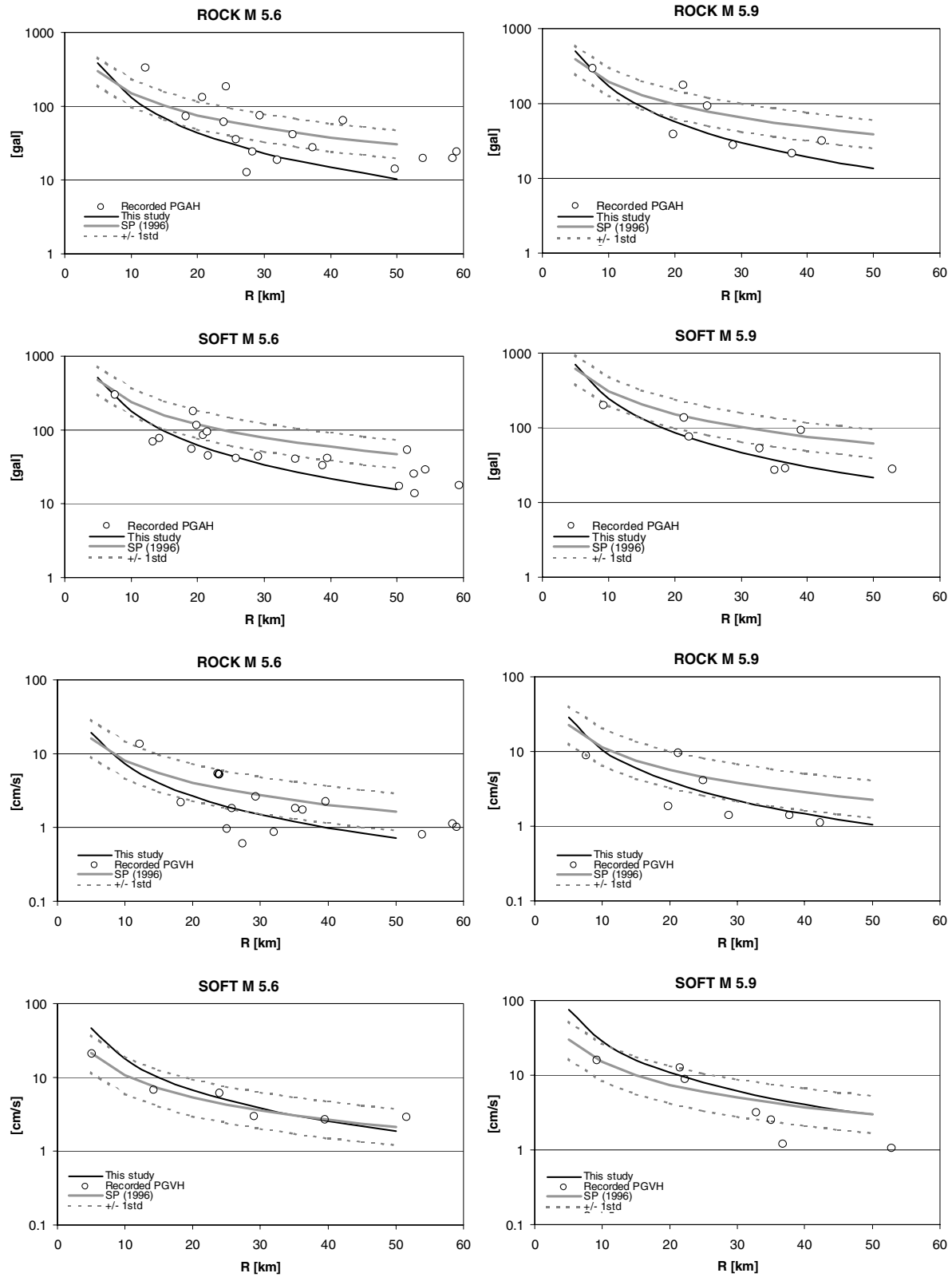


**Figure 8. Attenuation relations for peak ground acceleration and velocity at two assigned magnitudes.**

## REFERENCES

1. Amato A, et al. "The 1997 Umbria-Marche, Italy, earthquake sequence: a first look of the main shock and aftershock." *Geophys. Res. Lett.* 1998; 25: 2861-64.
2. Ambraseys N, Smit P, Sigbjornsson R, Suhadolc P, Margaritis B. "Internet-Site for European Strong-Motion Data." European Commission, Research-Directorate General, Environment and Climate Programme, 2002.
3. Anderson JG, Hough S. "A model for the shape of the Fourier amplitude spectrum of acceleration at high frequencies.", *Bull. Seismol. Soc. Am.*, 1984; 74: 1969-93.
4. Andrews DJ. "Objective determination of source parameters and similarity of earthquakes of different size." *Earthquake source mechanics*, S. Das, J. Boatwright, C. H. Sholz, *Geophysical Monograph* 37, M. Ewing, 1986, 6: 259-67.
5. Bernard P, Madariaga R. "A new asymptotic method for the modeling of near-field accelerograms." *Bull. Seism. Soc. Am.*, 1984; 74: 539-57.
6. Bindi D, Spallarossa D, Augliera P, Cattaneo M. "Source parameters estimated from the aftershocks of the 1997 Umbria - Marche (Italy) seismic sequence." *Bull. Seism. Soc. Am.*, 2001; 91: 448-55.
7. Bindi D, Castro RR, Franceschina G, Luzi L, Pacor F. "The 1997 - 1998 Umbria - Marche sequence (central Italy): Source, Path and Site effects estimated from strong motion data recorded in the epicentral area." *J. Geophys. Res.*, 2004, accepted.
8. Boore DM. "Stochastic simulation of high frequency ground motion based on seismological models of radiated spectra." *Bull. Seism. Soc. Am.*, 1983; 73: 1865-94.
9. Boore DM "Simulation of ground motion using the stochastic method." *Pure Appl. Geophys.*, 2003; 160: 635-76.
10. Brune JN. "Tectonic stress and the spectra of seismic shear waves from earthquakes." *J. Geophys. Res.*, 1970; 75: 4997-5009.
11. Castro RR, Anderson JG, Singh SK. "Site response, attenuation and source spectra of S waves along the Guerrero, México, subduction zone." *Bull. Seism. Soc. Am.*, 1990; 80: 1481-1503.
12. Castro RR, Monachesi G, Trojani L, Mucciarelli M, Frapiccini M. "An attenuation study using earthquakes from the 1997 Umbria-Marche sequence." *J. Seismol.*, 2002; 6: 43-59.
13. Castro RR, Monachesi G, Mucciarelli M, Trojani L, Pacor F. "P- and S-wave attenuation in the region of Marche, Italy." *Tectonophysics*, 1999; 302: 123-32
14. Castro RR, Pacor F, Bindi D, Franceschina G, Luzi L. "Site response of strong motion stations in the Umbria, central Italy, region." *Bull. Seism. Soc. Am.*, 2004; in press.
15. Ekström G, Morelli A, Boschi E, Dziewonski AM. "Moment tensor analysis of the central Italy earthquake sequence of September-October 1997." *Geophys. Res. Lett.*, 1998; 25: 1971-74.
16. Haskell NA. "The dispersion of surface waves on multilayered media." *Bull. Seism. Soc. Am.*, 1953; 43: 17-34.
17. Langston CA. "Structure under Mount Rainier, Washington, inferred from teleseismic body waves." *J. Geophys. Res.*, 1979; 84: 4749-62.
18. Lermo J, Chávez-García FJ. "Site effect evaluation using spectral ratios with only one station." *Bull. Seism. Soc. Am.*, 1993; 83: 1574-94.
19. Malagnini L, Herrmann RB. "Ground-motion scaling in the region of the 1997 Umbria-Marche earthquake (Italy)." *Bull. Seism. Soc. Am.*, 2000; 90: 1041-51.
20. Malagnini L, Herrmann RB, Di Bona M. "Ground-motion scaling in the Apennines (Italy)." *Bull. Seism. Soc. Am.*, 2000; 90: 1062-81.
21. Mendez A, Pacor F. "A study of the rupture characteristics of the 40s subevents of the 1980 Irpinia earthquake." *Annali di Geofisica*, 1994; 37: 1601-20.
22. Pacor F, Cultrera G, Mendez A, Cocco M. "Finite fault modeling of strong ground motions using a hybrid deterministic- stochastic approach." submitted to *Bull. Seism Soc. Am.*, 2003.

23. Paige CC, Saunders MA. "An algorithm for sparse linear equations and sparse least squares." *ACM Trans. Math. Softw.*, 1982; 8: 43-71.
24. Parolai S, Trojani L, Monachesi G, Frappicini M, Cattaneo M, Augliera P. "Hypocenter location accuracy and seismicity distribution in the central Apennines (Italy)." *J. Seismol.*, 2001; 5: 243-61.
25. Rovelli A, Bonamassa O, Cocco M, Di Bona M, Mazza S. "Scaling laws and spectral parameters of the ground motions in active extensional areas in Italy." *Bull. Seism. Soc. Am.*, 1988; 78: 530-60.
26. Sabetta F, Pugliese A. "Estimation of response spectra and simulation of non stationary earthquake ground motion." *Bull. Seism. Soc. Am.*, 1996; 86: 337-52.
27. Spudich P, Frazer LN. "Use of ray theory to calculate high-frequency radiation from earthquake sources having spatially variable rupture velocity and stress drop." *Bull. Seism. Soc. Am.*, 1984; 74: 2061-82.
28. S.S.N. Monitoring System Group. "The strong motion records of Umbria-Marche sequence (September 1997 - June 1998)." CD-ROM, 2002.
29. Thomson WT. "Transmission of elastic waves through a stratified solid medium." *J. Appl. Phys.*, 1950; 21: 89-93.